Challenge Journal of Structural Mechanics

Research Article

Three-dimensional static analysis of reinforced concrete cantilever beam using MATLAB Partial Differential Equation Toolbox

Olgun Köksal [a], Zeki Karaca [b], Erdem Türkeli [c,*]

[a] *Kavak Vocational School, Construction Department, Samsun University, 55850 Samsun, Türkiye*
[b] *Department of Civil Engineering, Ondokuz Mayıs University, 55270 Samsun, Türkiye*
[c] *Vocational School of Technical Sciences, Construction Department, Ordu University, 52200 Ordu, Türkiye*

ABSTRACT

Nowadays, three-dimensional (3D) solid model of the structures can be prepared by using computer aided design programs. There are many numerical methods for static, dynamic and temperature analysis of structural systems. The most preferred among these methods is the finite element method (FEM). In this method, the structural model with different geometry and boundary conditions should be solved by utilizing partial differential equations. Due to the long solution time while performing, finite element programs require computers with very good features. Therefore, analyses with desired features can be performed by using open source programs to shorten the duration of analysis. In this study, specifically, the static analysis of the selected reinforced concrete (RC) cantilever beam was carried out by using the open source MATLAB partial differential toolbox based on the FEM. Since the program used is open source, different concrete classes and finite element models were selected for the cited cantilever beam and static analyses were performed. As a result of the MATLAB partial differential toolbox analyses, the displacement, stress and deformation of the cantilever beam were obtained in 3D and compared with the ones obtained from ANSYS computer program.

ARTICLE INFO

Article history:
Received 6 May 2023
Revised 13 July 2023
Accepted 8 August 2023

Keywords:
Finite element method
Static analysis
Partial Differential Equation Toolbox
Cantilever beam

1. Introduction

With the development of computer technology in the last fifty years, modeling of structural systems and examining their behavior under external loads have attracted the attention of many researchers. Previously, the ideal conditions of the structural systems were determined and solutions were obtained with traditional analysis methods. Many new numerical methods have been the subject of theoretical research due to the fact that traditional methods solve plane problems, the results are approximate, the solution times are longer, they can work in certain geometries, and the choice of materials is limited (Argyris and Kelsey 1960). Among these methods, the FEM is one of the most preferred method today. FEM is a numerical method used to solve engineering and mathematical physics problems. By using this numerical method, problems in many fields such as structural mechanics and dynamics, fluid mechanics and dynamics, heat transfer, diffusion and electrostatics are solved. In the FEM method, it is desired to divide the engineering problem into small parts. Matrix solutions are realized by reflecting the contribution of these small parts from external effects and boundary conditions to the whole system. As a result of the solutions, displacement, stress and strain are obtained at a finite number of nodes (Kasımzade 2018).

FEM was first used in 1956 to solve space problems (Turner et al. 2012). With the development of computer technology, FEM started to take itself to the forefront in the 1970s (Bathe and Wilson 1976; Gallagher 1975; Oden and Sato 1967; Zienkiewicz 1972). Many researchers have prepared computer programs based on this method. Today, there are many finite element software

* *Corresponding author*. Tel.: +90-452-233-4865 ; Fax: +90-452-233-5230 ; E-mail address: erdemturkeli@odu.edu.tr (E. Türkeli)
ISSN: 2149-8024 / DOI: https://doi.org/10.20528/cjsmec.2023.03.003

prepared by both commercial companies and academicians (Kasımzade 2018). Since the program codes of commercial software for academic studies are generally not open source, academicians prefer open source software. In this study, linear static analysis of a RC cantilever beam was performed using MATLAB Partial Differential Equation Toolbox based on the FEM (MATLAB R2023a 2023). By selecting different strength classes for concrete and different types of finite elements, displacement, stress and strain results are presented.

2. Material and Method

2.1. MATLAB Partial Differential Equation Toolbox

The Partial Differential Equation Toolbox (PDE Toolbox) (Fig. 1) provides functions for solving structural mechanics, heat transfer, and general partial differential equations (PDEs) using the finite element method (MATLAB R2023a 2023) .

Features of this cited toolbox (MATLAB R2023a 2023);

- It can be used to calculate deformations and stresses.
- For modeling the dynamics and vibration of the structure, the toolbox has a time-integrating solver directly.
- It can analyze the structural properties of a component by performing modal analysis to find natural frequencies and mode shapes.
- It can model conductive heat transfer problems to calculate heat distributions, heat flow and heat flow rates over surfaces.
- It can also solve standard problems such as diffusion, electrostatics, magnetostatics and special PDEs.
- Imports 2D and 3D geometries using mesh data.
- It can automatically create meshes with triangular and tetrahedral elements.

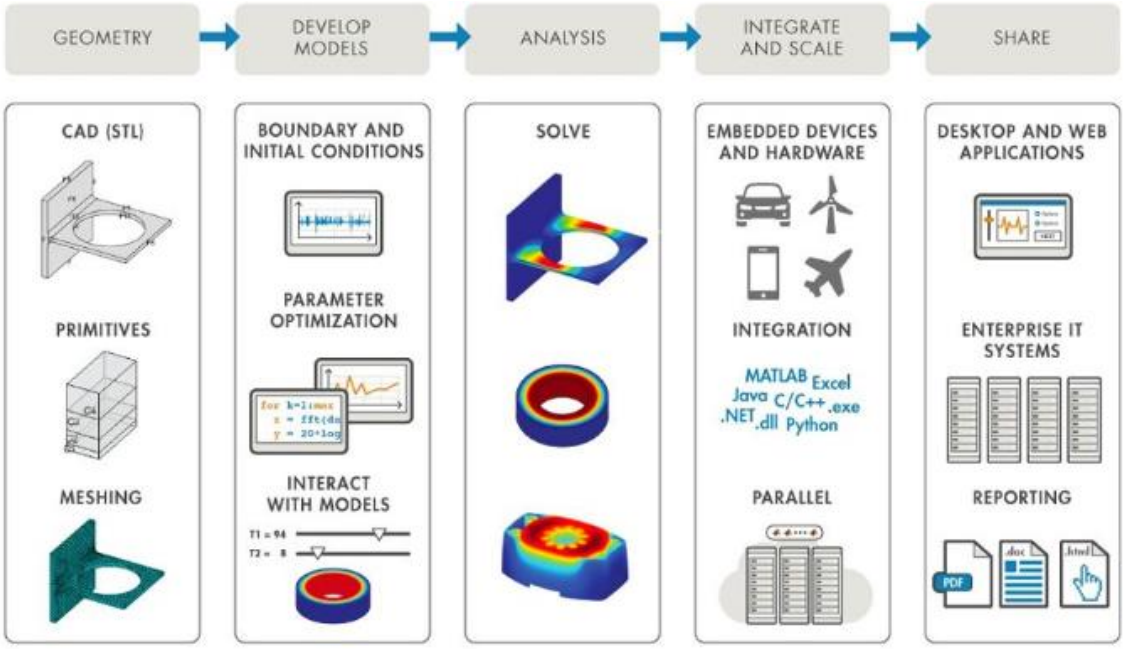

Fig. 1. The flowchart of PDE Toolbox (MATLAB R2023a 2023).

The PDE toolbox calculates equations in the form given below (MATLAB R2023a 2023).

$$m\frac{\partial^2 u}{\partial t^2} + d\frac{\partial u}{\partial t} \cdot \nabla \cdot (c\nabla u) + au = f \quad (1)$$

$$\nabla \cdot (c\nabla u) + au = \lambda du \quad (2)$$

$$\nabla \cdot (c\nabla u) + au = \lambda^2 mu \quad (3)$$

Eq. (3) solves eigenvalue problems. When solving PDEs, there are two boundary choices for each edge or face. Dirichlet boundary conditions performs the solution equation at the edge or surface.

$$hu = r \quad (4)$$

where, h and r are denoting 3D (x, y, z) space functions. Generalized Neumann boundary conditions performs the solution equation at the edge or surface.

$$\vec{n} \cdot (c\nabla u) + qu = g \quad (5)$$

$\vec{n}$ is denoting the unit normal vector. q and g are functions defined in $\partial\Omega$ depending on (x, y, z) in 3D space.

2.2. Linear equations of elasticity

In linear elasticity, the stiffness matrix of an isotropic material depends on two parameters, E, representing Young's modulus and ν, Poisson's ratio. Equilibrium equation in static condition is given in Eq. (6).

$$-\nabla.\sigma = f \quad (6)$$

The relationship between linearized small displacements and strains is given with Eq. (7).

$$\varepsilon = \frac{1}{2}(\nabla u + \nabla u^T) \tag{7}$$

The angular momentum equilibrium shows that the stress is symmetrical.

$$\sigma_{ij} = \sigma_{ji} \tag{8}$$

According to the linear elasticity theory, the relationship between stress and strain is as follows.

$$\begin{bmatrix}\sigma_{11}\\ \sigma_{22}\\ \sigma_{33}\\ \sigma_{23}\\ \sigma_{13}\\ \sigma_{12}\end{bmatrix} = \frac{E}{(1-\nu)(1-2\nu)}\begin{bmatrix}1-\nu & \nu & \nu & 0 & 0 & 0\\ \nu & 1-\nu & \nu & 0 & 0 & 0\\ \nu & \nu & 1-\nu & 0 & 0 & 0\\ 0 & 0 & 0 & 1-2\nu & 0 & 0\\ 0 & 0 & 0 & 0 & 1-2\nu & 0\\ 0 & 0 & 0 & 0 & 0 & 1-2\nu\end{bmatrix}\begin{bmatrix}\varepsilon_{11}\\ \varepsilon_{22}\\ \varepsilon_{33}\\ \varepsilon_{23}\\ \varepsilon_{13}\\ \varepsilon_{12}\end{bmatrix} \tag{9}$$

If written in expanded form, Eq. (10) is obtained in which • shows the symmetricity.

$$\begin{bmatrix}\sigma_{11}\\ \sigma_{12}\\ \sigma_{13}\\ \sigma_{21}\\ \sigma_{22}\\ \sigma_{23}\\ \sigma_{31}\\ \sigma_{32}\\ \sigma_{33}\end{bmatrix} = \frac{E}{(1-\nu)(1-2\nu)}\begin{bmatrix}1-\nu & 0 & 0 & 0 & \nu & 0 & 0 & 0 & \nu\\ \bullet & 1-2\nu & 0 & 0 & 0 & 0 & 0 & 0 & 0\\ \bullet & \bullet & 1-2\nu & 0 & 0 & 0 & 0 & 0 & 0\\ \bullet & \bullet & \bullet & 1-2\nu & 0 & 0 & 0 & 0 & 0\\ \bullet & \bullet & \bullet & \bullet & 1-\nu & 0 & 0 & 0 & \nu\\ \bullet & \bullet & \bullet & \bullet & \bullet & 1-2\nu & 0 & 0 & 0\\ \bullet & \bullet & \bullet & \bullet & \bullet & \bullet & 1-2\nu & 0 & 0\\ \bullet & \bullet & \bullet & \bullet & \bullet & \bullet & \bullet & 1-2\nu & 0\\ \bullet & \bullet & \bullet & \bullet & \bullet & \bullet & \bullet & \bullet & 1-\nu\end{bmatrix} \tag{10}$$

2.3. Three-dimensional linear equations of elasticity

If Eq. (6) is written for MATLAB PDE Toolbox, Eq. (11) is obtained.

$$-\nabla(c \otimes \nabla u) = f \tag{11}$$

$$\varepsilon = \frac{1}{2}(\nabla u + \nabla u^T) \tag{12}$$

Strain depends on both ∇u and its transpose. If it is necessary to convert this from strain to ∇u, and the column is written in vector form, Eq. (13) can be obtained.

$$\nabla u = \begin{bmatrix}\partial u_x/\partial x\\ \partial u_x/\partial y\\ \partial u_x/\partial z\\ \partial u_y/\partial x\\ \partial u_y/\partial y\\ \partial u_y/\partial z\\ \partial u_z/\partial x\\ \partial u_z/\partial y\\ \partial u_z/\partial z\end{bmatrix} \tag{13}$$

After that, the deformation-displacement relationship can be written in Eqs. (14)-(20):

$$\varepsilon = \begin{bmatrix}1 & 0 & 0 & 0 & 0 & 0 & 0 & 0 & 0\\ 0 & 1/2 & 0 & 1/2 & 0 & 0 & 0 & 0 & 0\\ 0 & 0 & 1/2 & 0 & 0 & 0 & 1/2 & 0 & 0\\ 0 & 1/2 & 0 & 1/2 & 0 & 0 & 0 & 0 & 0\\ 0 & 0 & 0 & 0 & 1 & 0 & 0 & 0 & 0\\ 0 & 0 & 0 & 0 & 0 & 1/2 & 0 & 0 & 0\\ 0 & 0 & 1/2 & 0 & 0 & 0 & 1/2 & 0 & 0\\ 0 & 0 & 0 & 0 & 0 & 1/2 & 0 & 1/2 & 0\\ 0 & 0 & 0 & 0 & 0 & 0 & 0 & 0 & 1\end{bmatrix} \nabla u \equiv A\nabla u \tag{14}$$

$$\sigma = \frac{E}{(1-\nu)(1-2\nu)} \begin{bmatrix} 1-\nu & 0 & 0 & 0 & \nu & 0 & 0 & 0 & \nu \\ \bullet & 1-2\nu & 0 & 0 & 0 & 0 & 0 & 0 & 0 \\ \bullet & \bullet & 1-2\nu & 0 & 0 & 0 & 0 & 0 & 0 \\ \bullet & \bullet & \bullet & 1-2\nu & 0 & 0 & 0 & 0 & 0 \\ \bullet & \bullet & \bullet & \bullet & 1-\nu & 0 & 0 & 0 & \nu \\ \bullet & \bullet & \bullet & \bullet & \bullet & 1-2\nu & 0 & 0 & 0 \\ \bullet & \bullet & \bullet & \bullet & \bullet & \bullet & 1-2\nu & 0 & 0 \\ \bullet & \bullet & \bullet & \bullet & \bullet & \bullet & \bullet & 1-2\nu & 0 \\ \bullet & \bullet & \bullet & \bullet & \bullet & \bullet & \bullet & \bullet & 1-\nu \end{bmatrix} A\nabla u \tag{15}$$

$$\sigma = \frac{E}{(1-\nu)(1-2\nu)} \begin{bmatrix} 1-\nu & 0 & 0 & 0 & \nu & 0 & 0 & 0 & \nu \\ 0 & 1/2-\nu & 0 & 1/2-\nu & 0 & 0 & 0 & 0 & 0 \\ 0 & 0 & 1/2-\nu & 0 & 0 & 0 & 1/2-\nu & 0 & 0 \\ 0 & 1/2-\nu & 0 & 1/2-\nu & 0 & 0 & 0 & 0 & 0 \\ \nu & 0 & 0 & 0 & 1-\nu & 0 & 0 & 0 & \nu \\ 0 & 0 & 0 & 0 & 0 & 1-2\nu & 0 & 1-2\nu & 0 \\ 0 & 0 & 1/2-\nu & 0 & 0 & 0 & 1-2\nu & 0 & 0 \\ 0 & 0 & 0 & 0 & 0 & 1/2-\nu & 0 & 1-2\nu & 0 \\ \nu & 0 & 0 & 0 & \nu & 0 & 0 & 0 & 1-\nu \end{bmatrix} \nabla u \tag{16}$$

$$\mu = \frac{E}{2(1+\nu)} \tag{17}$$

$$\lambda = \frac{E\nu}{(1+\nu)(1-2\nu)} \tag{18}$$

$$2\mu + \lambda = \frac{E(1-\nu)}{(1+\nu)(1-2\nu)} \tag{19}$$

Equalities are obtained. If rearranged accordingly, Eq. (20) can be obtained.

$$\sigma = \begin{bmatrix} 2\mu+\lambda & 0 & 0 & 0 & \lambda & 0 & 0 & 0 & \lambda \\ 0 & \mu & 0 & \mu & 0 & 0 & 0 & 0 & 0 \\ 0 & 0 & \mu & 0 & 0 & 0 & \mu & 0 & 0 \\ 0 & \mu & 0 & \mu & 0 & 0 & 0 & 0 & 0 \\ \lambda & 0 & 0 & 0 & 2\mu+\lambda & 0 & 0 & 0 & \lambda \\ 0 & 0 & 0 & 0 & 0 & \mu & 0 & \mu & 0 \\ 0 & 0 & \mu & 0 & 0 & 0 & \mu & 0 & 0 \\ 0 & 0 & 0 & 0 & 0 & \mu & 0 & \mu & 0 \\ \lambda & 0 & 0 & 0 & \lambda & 0 & 0 & 0 & 2\mu+\lambda \end{bmatrix} \nabla u \equiv c\nabla u \tag{20}$$

The equation for the von Mises yield criterion is given below (McDowell and Ellis 1993; Jones 2009).

$$\sigma_v = \sqrt{\frac{1}{2}\left[\left(\sigma_{xx}-\sigma_{yy}\right)^2 + \left(\sigma_{yy}-\sigma_{zz}\right)^2 + (\sigma_{zz}-\sigma_{xx})^2 + 6\left(\sigma_{xy}^2+\sigma_{yz}^2+\sigma_{zx}^2\right)^2\right]} \tag{21}$$

$$\varepsilon_v = \frac{1}{\sqrt{2}(1+\upsilon)}\sqrt{\left[\left(\varepsilon_{xx}-\varepsilon_{yy}\right)^2 + \left(\varepsilon_{yy}-\varepsilon_{zz}\right)^2 + (\varepsilon_{zz}-\varepsilon_{xx})^2 + \frac{3}{2}\left(\gamma_{xy}^2+\gamma_{yz}^2+\gamma_{zx}^2\right)^2\right]} \tag{22}$$

2.4. RC cantilever beam

Cantilever beams are often needed in civil engineering applications. As an example, a RC cantilever beam was chosen as in Fig. 2 (Doğangün 2020). The RC cantilever beam in Fig. 2 has a rectangular section with a span of L=2.00m, a width of b=0.25m, and a height of h=0.50m. The cantilever beam is loaded with a distributed load of q=100kN/m. Point A is fixed support, point B has no support.

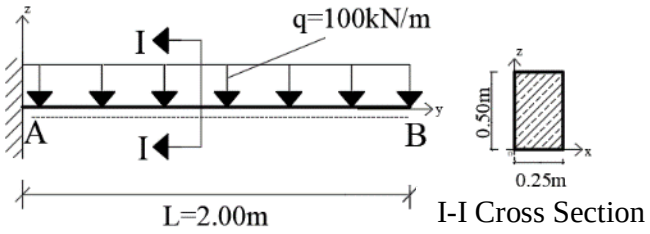

Fig. 2. Geometric properties and loading conditions of RC cantilever beam.

The material properties to be used for the static analysis of the cited RC cantilever beam are also given in Table 1.

In Fig. 3(a), the 3D solid model of the cantilever beam was created with the MATLAB PDE toolbox. The material properties of the RC cantilever beam are coded according to Table 1. Fig. 3(b) shows 3D linear tetrahedral solid finite element modeling for cantilever beam constructed in ANSYS (2016). The finite element model of the cantilever beam provided in Fig. 3(b) has a total of 966 nodes and 3852 finite elements.

Table 1. Material properties of RC cantilever beam (UNE EN 1992-1-2:2011/A1:2021 Eurocode 2: n.d.).

Concrete class	Characteristic cylinder compressive strength (MPa)	Characteristic cube compressive strength (MPa)	Elasticity module (MPa)	Poisson ratio	Unit volume weight (kN/m³)
C25/30	25	30	31476	0.2	25
C30/37	30	37	32837	0.2	25
C35/45	35	45	34077	0.2	25
C40/50	40	50	35220	0.2	25
C45/55	45	55	36283	0.2	25

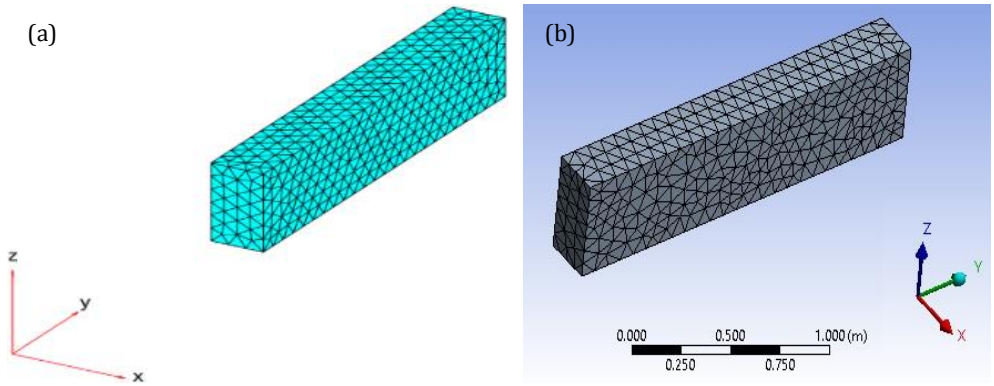

Fig. 3. RC cantilever beam: (a) 3D solid model (MATLAB); (b) mesh with linear tetrahedral solid elements (ANSYS).

3. Findings and Discussion

In this section of the study, displacement, deformation and stress distributions obtained for different concrete classes (using MATLAB PDE Toolbox) of the cited RC cantilever beam are provided in Figs. 4-13.

In addition, for different concrete classes, the separate analysis results given in Figs. 4-13 are provided collectively in Figs. 14-21.

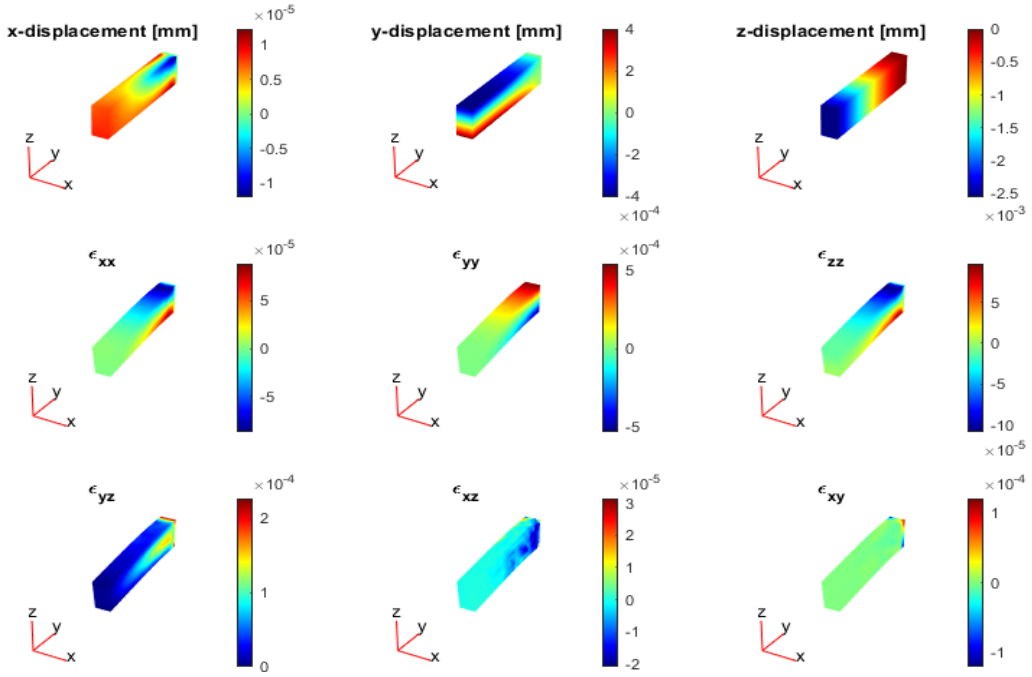

Fig. 4. Displacement and deformation results of C25/30 RC cantilever beam.

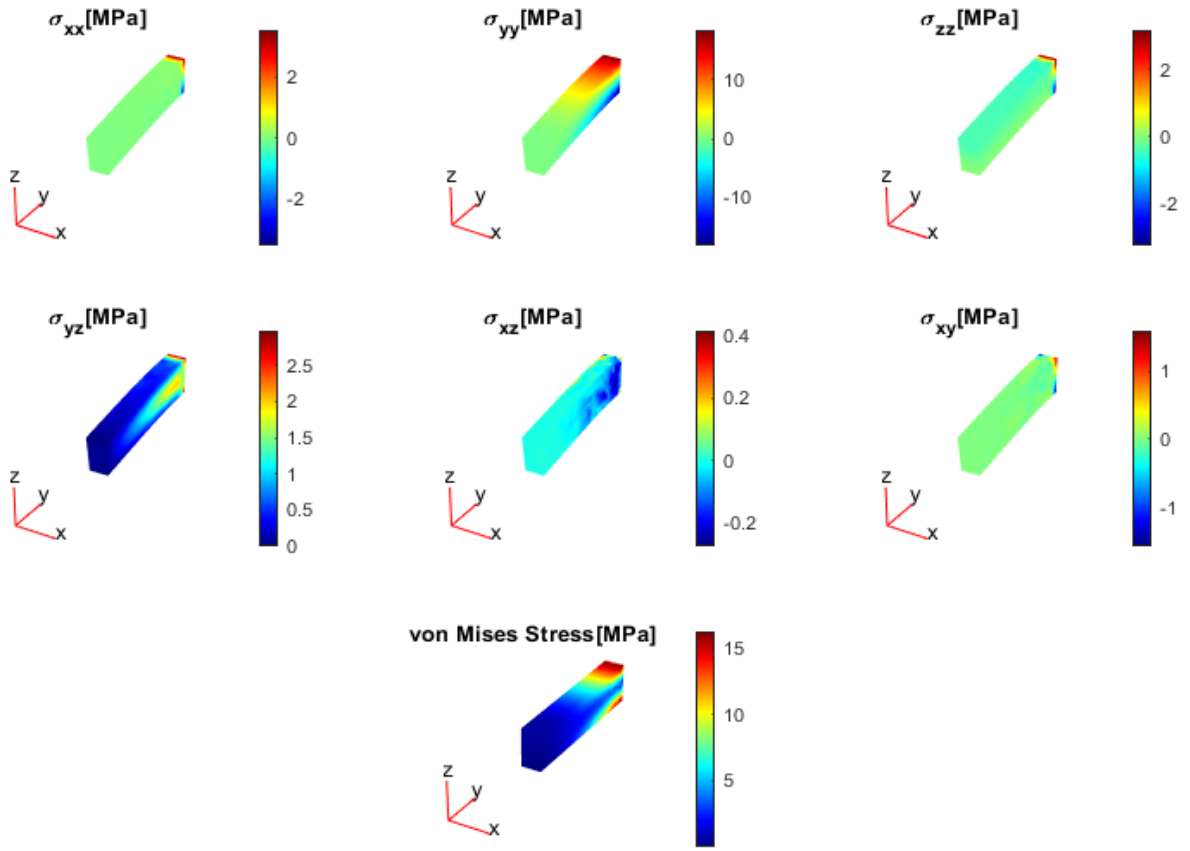

Fig. 5. Stress results of C25/30 RC cantilever beam.

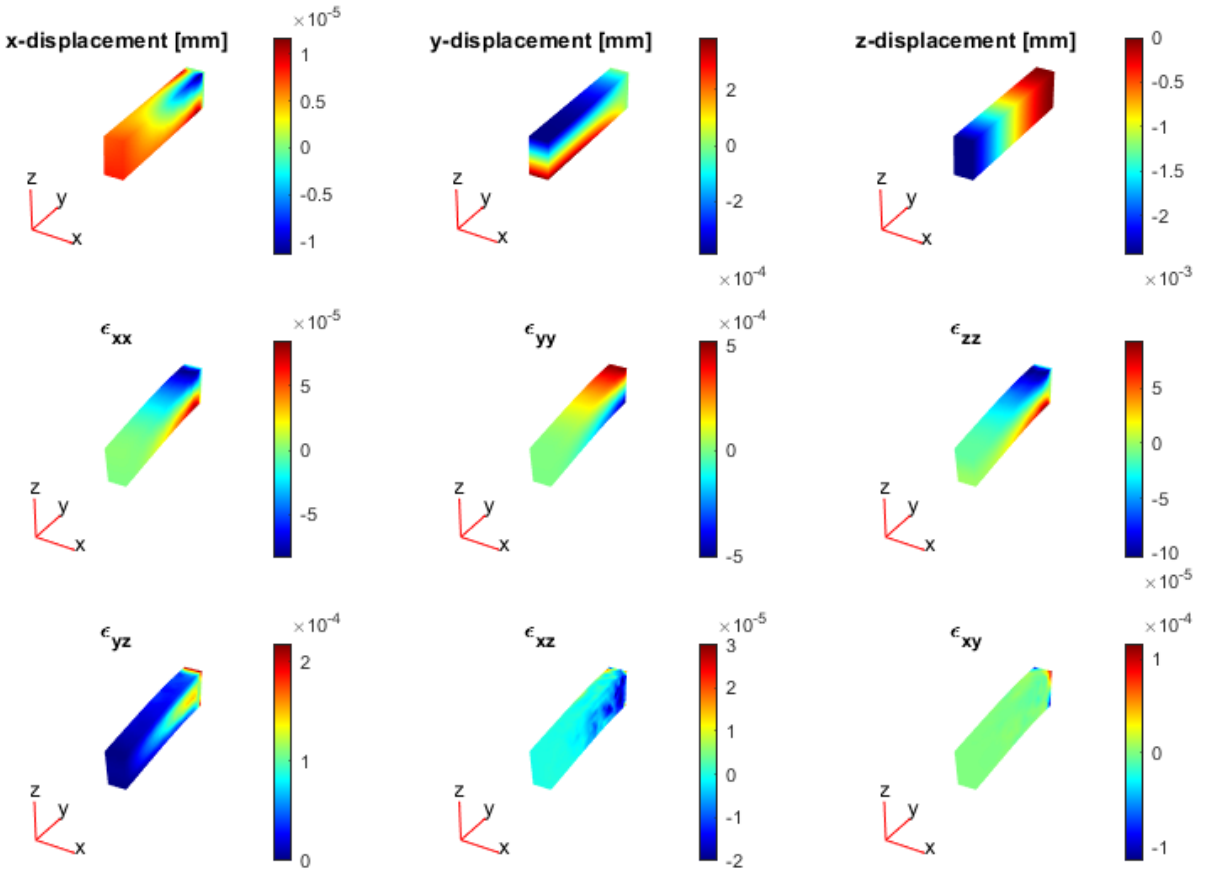

Fig. 6. Displacement and deformation results of C30/37 RC cantilever beam.

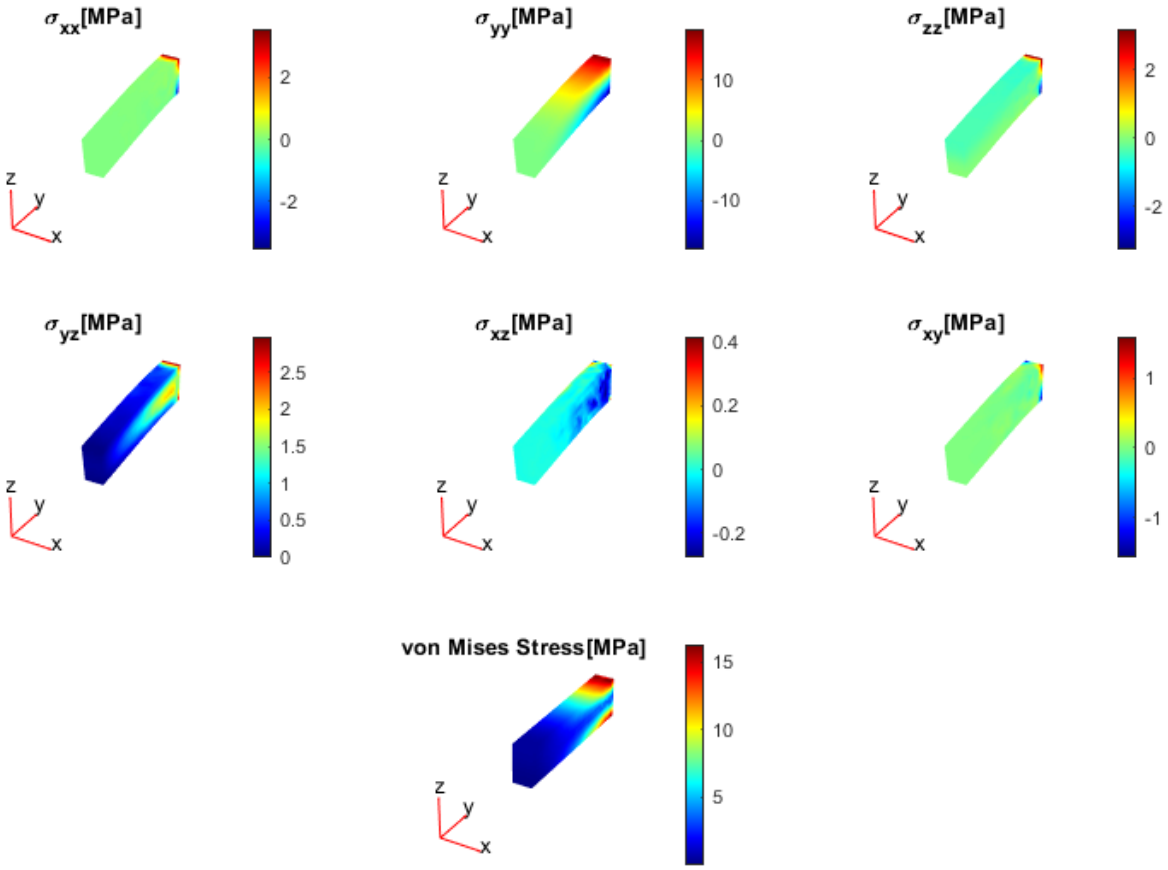

Fig. 7. Stress results of C30/37 RC cantilever beam.

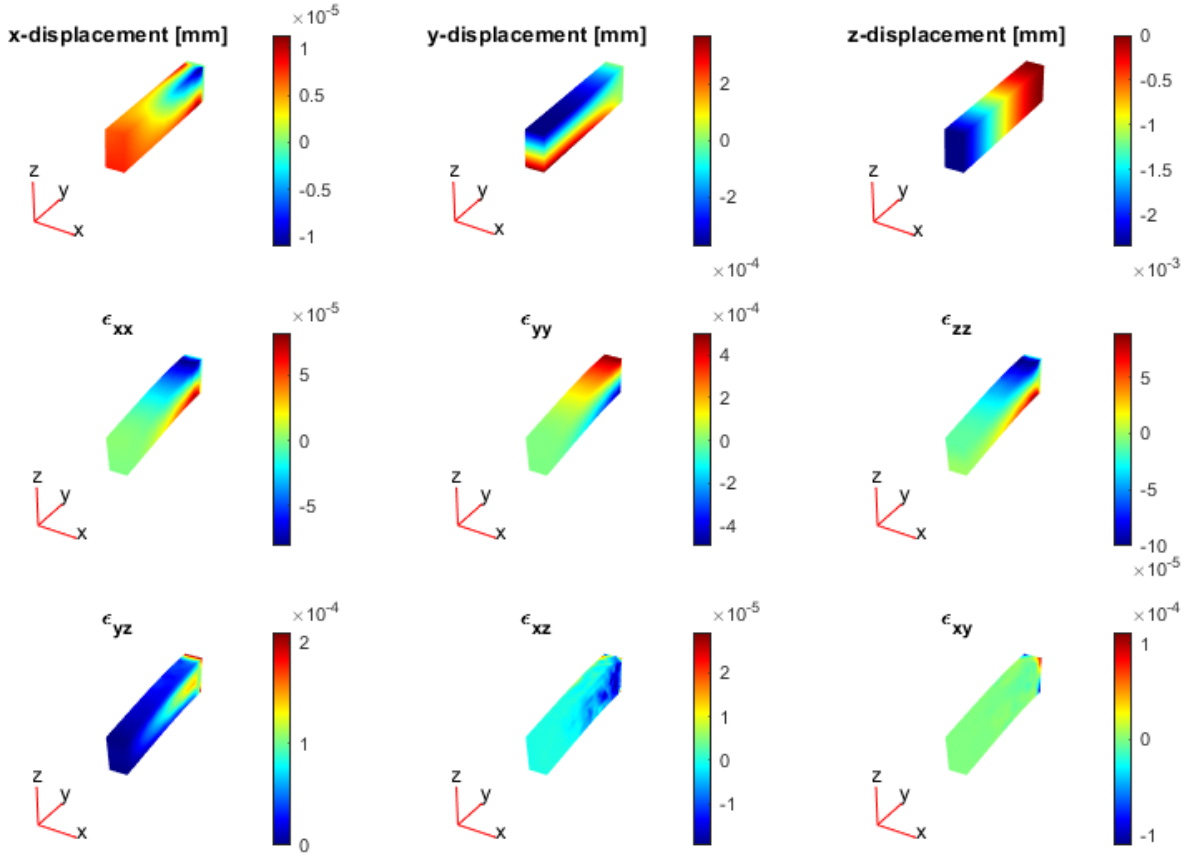

Fig. 8. Displacement and deformation results of C35/45 RC cantilever beam.

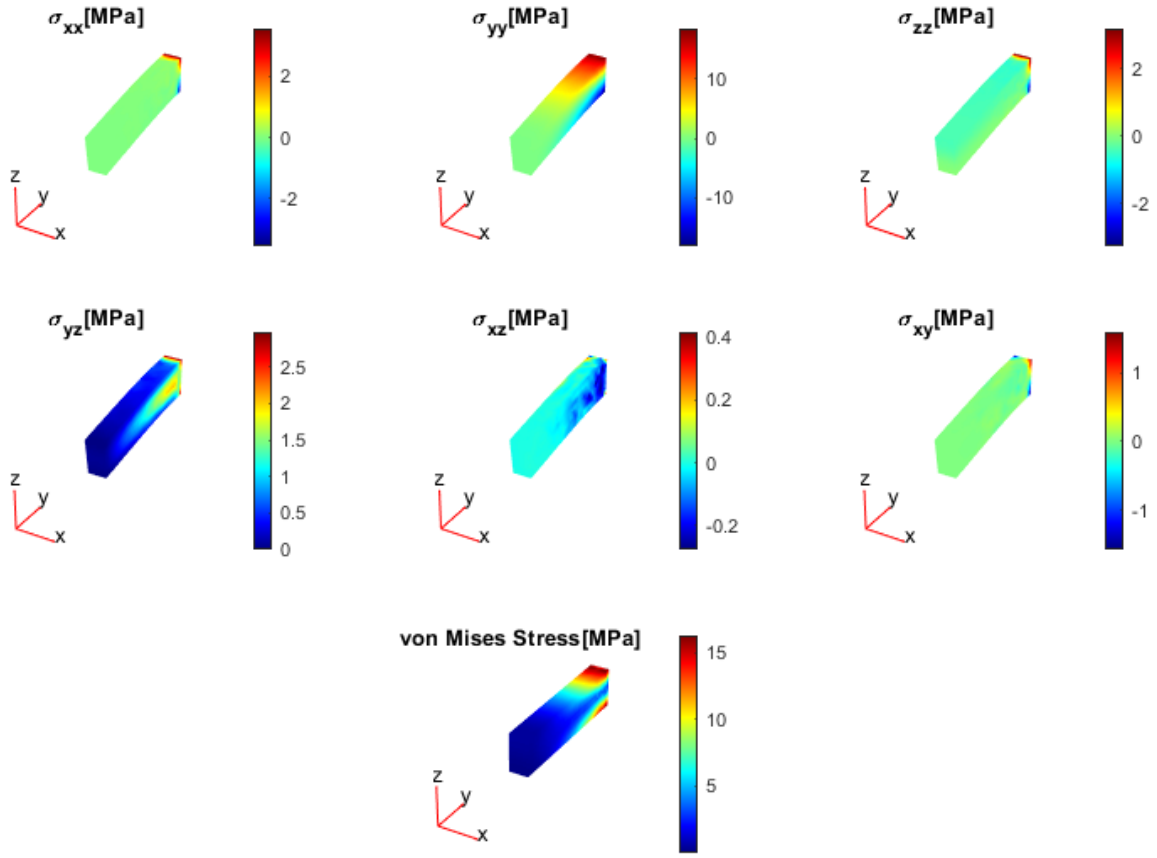

Fig. 9. Stress results of C35/45 RC cantilever beam.

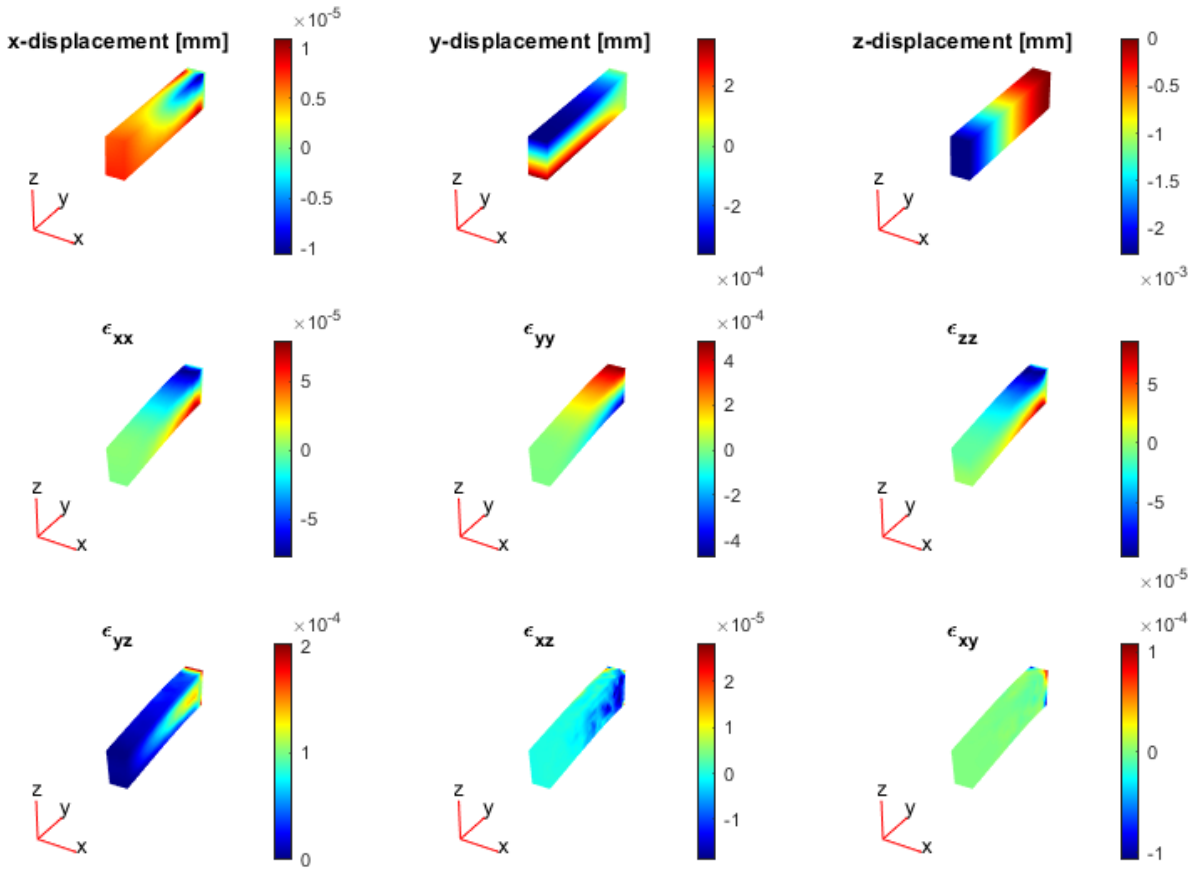

Fig. 10. Displacement and deformation results of C40/50 RC cantilever beam.

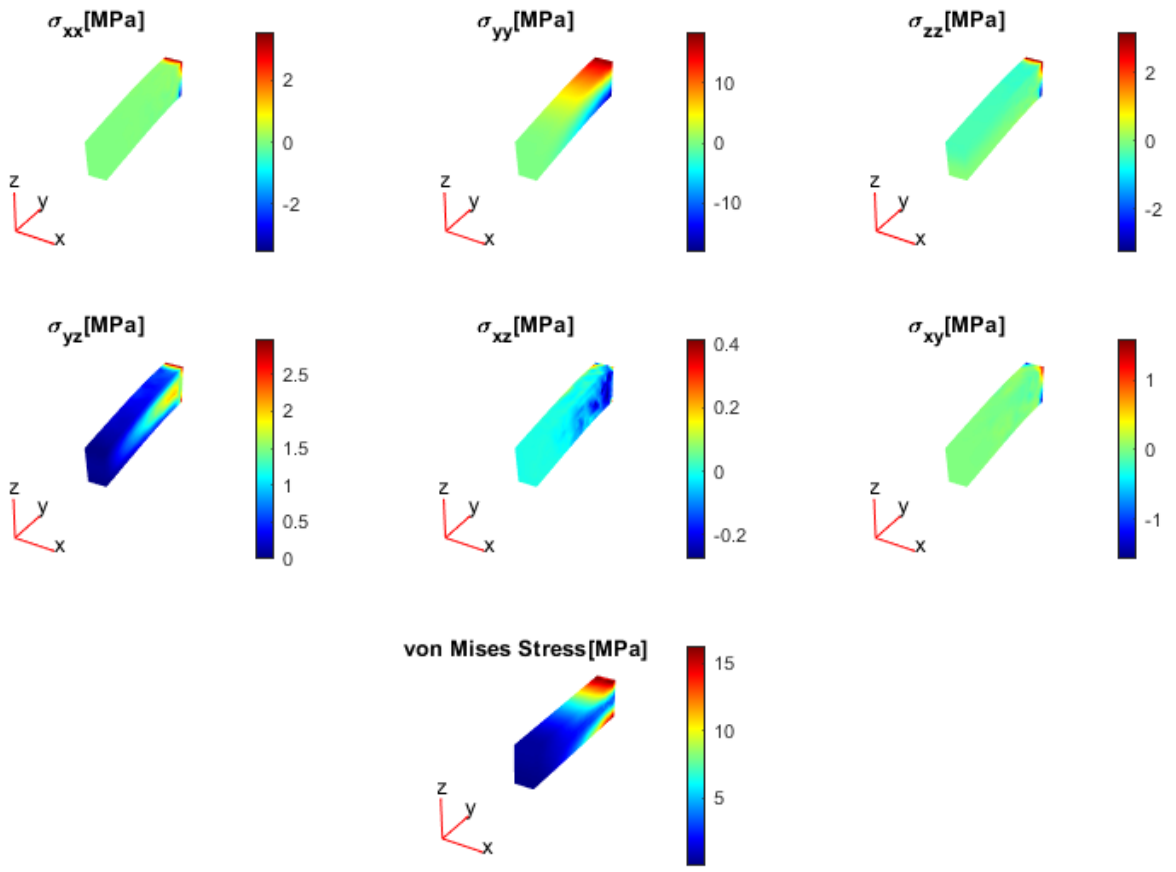

Fig. 11. Stress results of C40/50 RC cantilever beam.

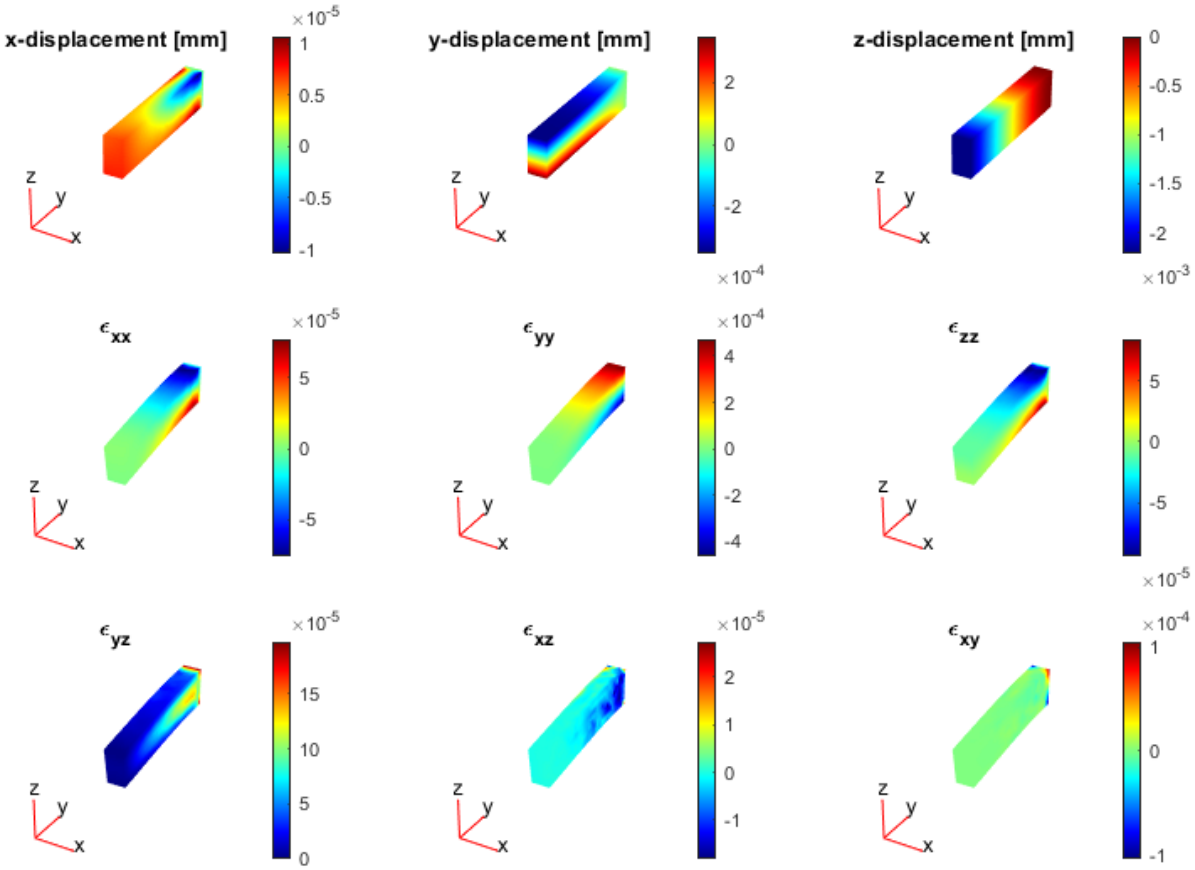

Fig. 12. Displacement and deformation results of C45/55 RC cantilever beam.

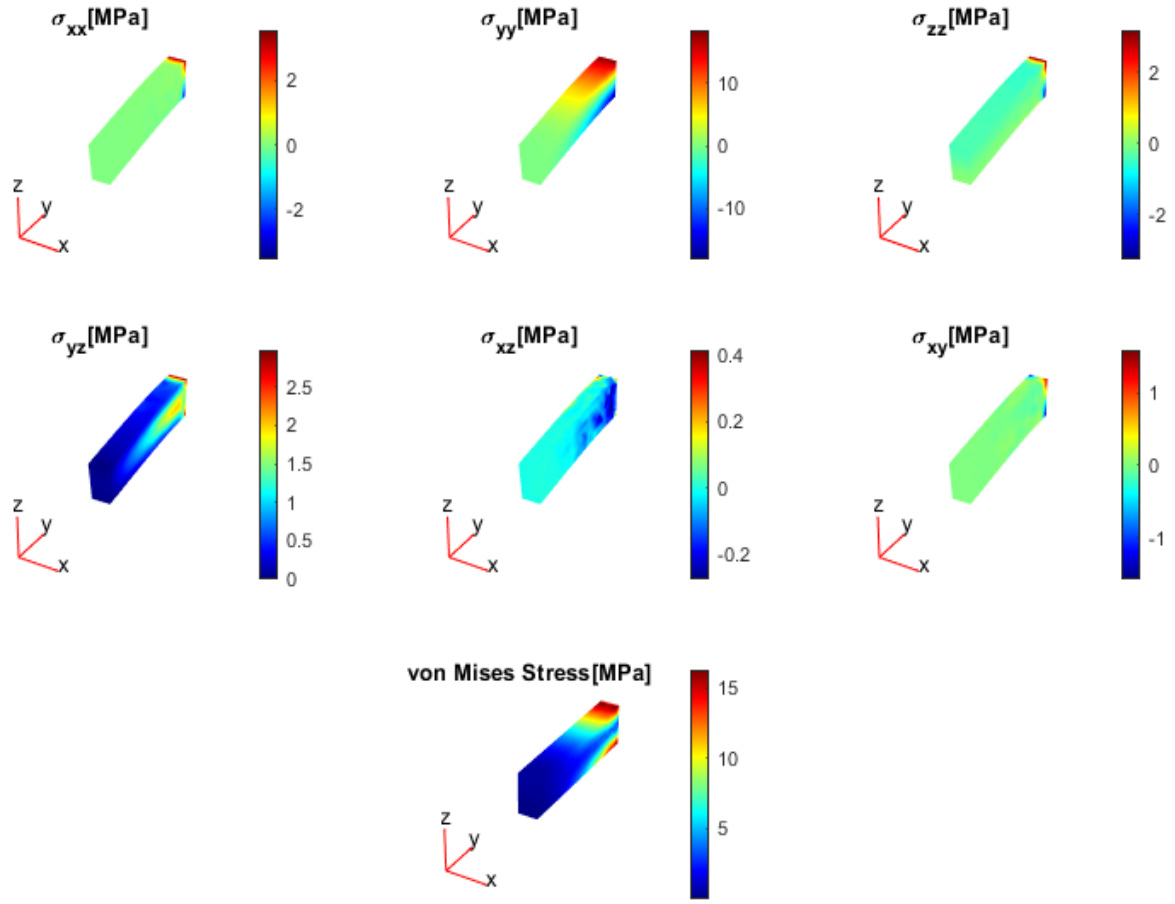

Fig. 13. Stress results of C45/55 RC cantilever beam.

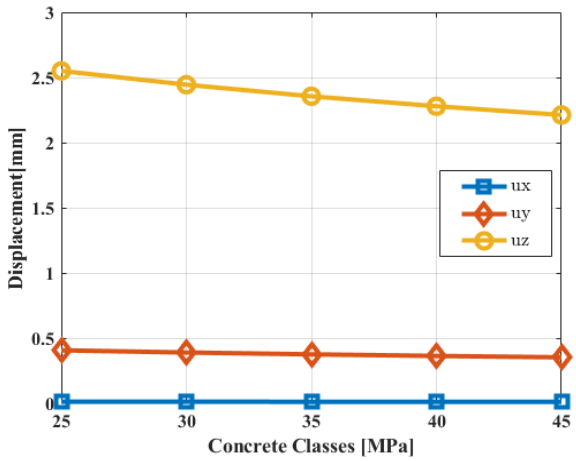

Fig. 14. The relationship of displacement (in the direction of z) with the concrete class.

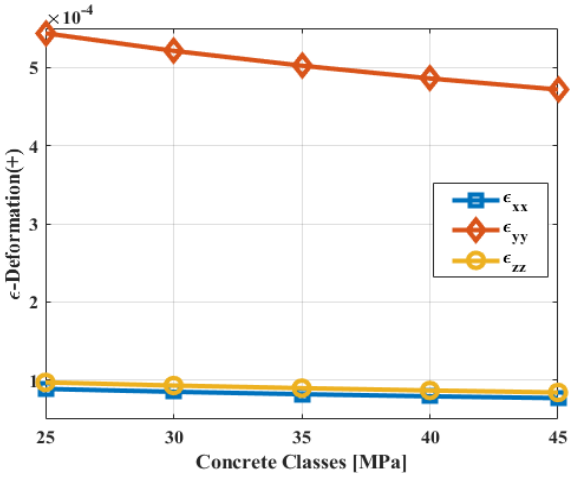

Fig. 15. The relationship of deformation (elongation in the direction of y) with the concrete class.

By examining Figs. 4, 6, 8, 10, 12 and 14 together, it can be clearly seen that the displacement in the z-axis direction (the distributed loading direction) decreases with the increase of the compressive strength of the concrete.

By examining Figs. 4, 6, 8, 10, 12 and 15 together, it can be clearly identified that the deformation (elongation) in the y-axis direction decreases with the increase in the compressive strength of the concrete.

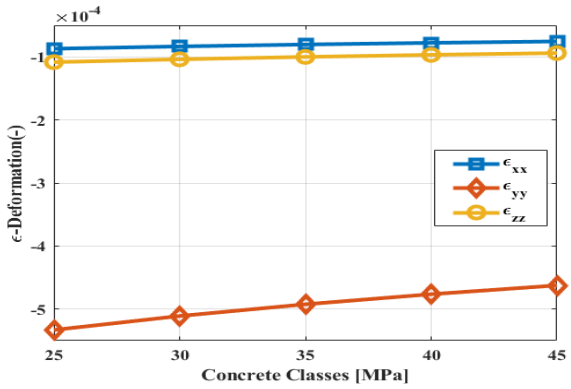

Fig. 16. The relationship of deformation (shortening in the direction of *y*) with the concrete class.

By examining Figs. 4, 6, 8, 10, 12 and 16 together, it can be deducted that the deformation (shortening) in the *y*-axis direction decreases with the increase in the compressive strength of the concrete.

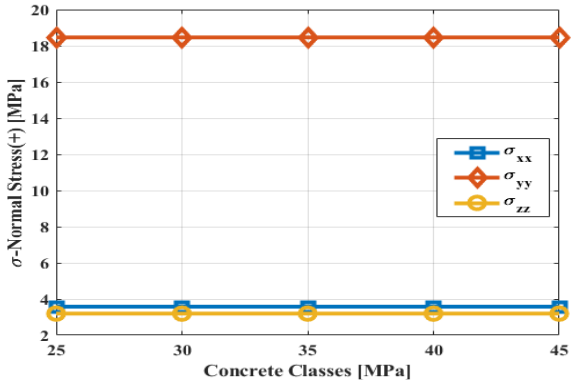

Fig. 17. Normal stress (tensile in bending) relationship with concrete classes.

Examining Figs. 5, 7, 9, 11, 13 and 17 together revealed that the normal stress (tensile in bending) in the y-axis direction remains constant with the increase in the compressive strength of the concrete.

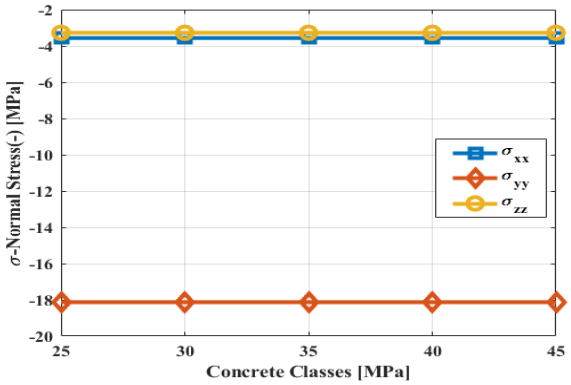

Fig. 18. Normal stress (compression in bending) relationship with concrete classes.

Examining Figs. 5, 7, 9, 11, 13 and 18 together, revealed that the normal stress (compression in bending) in the *y*-axis direction remains constant with the increase in the compressive strength of the concrete.

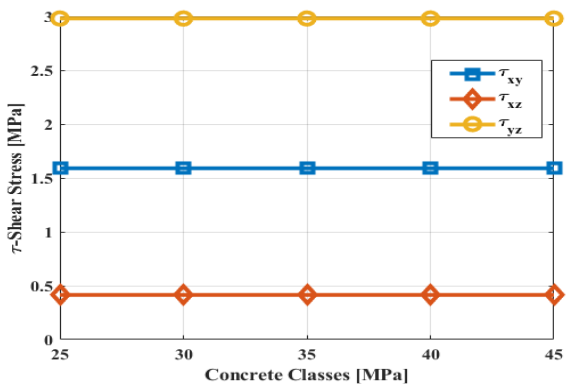

Fig. 19. Shear stress (positive) relationship with concrete classes.

By examining Fig. 5, 7, 9, 11, 13 and 19 together, revealed that the shear stress (positive) in the *xy*-axis direction remains constant with the increase in the compressive strength of the concrete.

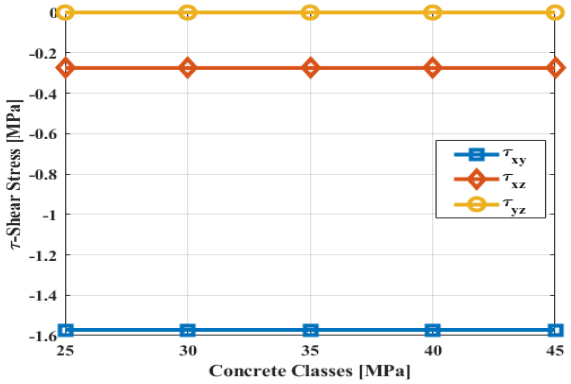

Fig. 20. Shear stress (negative) relationship with concrete classes.

By examining Fig. 5, 7, 9, 11, 13 and 20 together, it can be deducted that the shear stress (negative) in the *xy*-axis direction remains constant with the increase in the compressive strength of the concrete.

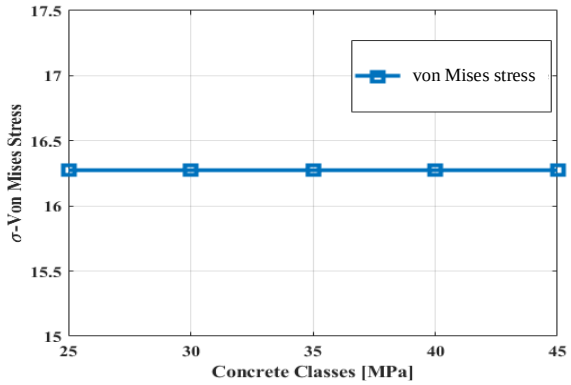

Fig. 21. von Mises stress relationship with concrete classes.

By examining Figs. 5, 7, 9, 11, 13 and 21 together, von Mises stresses seem to remain constant with the increase of the compressive strength of the concrete.

A comparison of MATLAB PDE Toolbox results and ANSYS results are provided in Tables 2-6. By examining the results for all concrete classes, it is seen that the displacement, deformation and stress values obtained from both methods are very close to each other.

Table 2. Comparison of MATLAB PDE Toolbox and ANSYS results (for C25/30 concrete class).

	MATLAB	ANSYS
Largest displacement (u_z)	2.56 mm	2.56 mm
Largest deformation (ε_{yy})	0.00054	0.00055
Largest normal stress (σ_{yy})	18.46 MPa	18.57 MPa
Largest shear stress (τ_{yz})	2.97 MPa	2.92 MPa
Largest von Mises stress	16.27 MPa	16.14 MPa
Largest von Mises strain	0.00052	0.00052

Table 3. Comparison of MATLAB PDE Toolbox and ANSYS results (for C30/37 concrete class).

	MATLAB	ANSYS
Largest displacement (u_z)	2.44 mm	2.46 mm
Largest deformation (ε_{yy})	0.000521	0.00054
Largest normal stress (σ_{yy})	18.46 MPa	18.57 MPa
Largest shear stress (τ_{yz})	2.97 MPa	2.92 MPa
Largest von Mises stress	16.27 MPa	16.15 MPa
Largest von Mises strain	0.000495	0.00049

Table 4. Comparison of MATLAB PDE Toolbox and ANSYS results (for C35/45 concrete class).

	MATLAB	ANSYS
Largest displacement (u_z)	2.35 mm	2.37 mm
Largest deformation (ε_{yy})	0.000502	0.00052
Largest normal stress (σ_{yy})	18.46 MPa	18.57 MPa
Largest shear stress (τ_{yz})	2.97 MPa	2.92 MPa
Largest von Mises stress	16.27 MPa	16.15 MPa
Largest von Mises strain	0.00047	0.00047

Table 5. Comparison of MATLAB PDE Toolbox and ANSYS results (for C40/50 concrete class).

	MATLAB	ANSYS
Largest displacement (u_z)	2.27 mm	2.29 mm
Largest deformation (ε_{yy})	0.000485	0.00050
Largest normal stress (σ_{yy})	18.46 MPa	18.57 MPa
Largest shear stress (τ_{yz})	2.97 MPa	2.92 MPa
Largest von Mises stress	16.27 MPa	16.15 MPa
Largest von Mises strain	0.00046	0.00046

Table 6. Comparison of MATLAB PDE Toolbox and ANSYS results (for C45/55 concrete class).

	MATLAB	ANSYS
Largest displacement (u_z)	2.21 mm	2.22 mm
Largest deformation (ε_{yy})	0.0004716	0.00048
Largest normal stress (σ_{yy})	18.46 MPa	18.57 MPa
Largest shear stress (τ_{yz})	2.97 MPa	2.92 MPa
Largest von Mises stress	16.27 MPa	16.15 MPa
Largest von Mises strain	0.000448	0.00045

In 15.4.9.a matter of Turkish Building Earthquake Code 2018 (Turkish Building Earthquake Code-2018 n.d.), it is specified that "Maximum compressive strain (deformation) of concrete can be taken as 0.0035 and maximum strain (deformation) of reinforcing steel can be taken as 0.01". By examining Tables 2-6, it can be seen that the deformations are below the limit values of the cited code. In addition, von Mises stresses are below the boundary stress values of the concrete (UNE EN 1992-1-2:2011/A1:2021 Eurocode 2: n.d.).

4. Conclusions

In this study, 3D static analyzes of a RC cantilever beam were carried out according to different concrete classes. Modeling and analysis of the cited beam were carried out using open source codes with the MATLAB PDE toolbox based on the FEM, and the results were compared with the ANSYS computer program. As a result of the structural analysis, displacements, deformations and stresses were obtained. It has been observed that the displacements, deformations and stresses do not exceed the standard limit values. By comparing the vertical displacement in the z-axis direction between the lowest concrete class (C25/30) and the highest concrete class (C45/50), a decrease of 18.18% has been found. Likewise, when a comparison is made for deformation (elongation) and deformation (shortening) in the y-axis direction, there is a 15.27% reduction. Moreover, when a comparison is made for normal stress (tensile and compressive in bending), shear stress and von Mises stresses, it can be identified that the values remain constant. In addition, same structural analyzes were carried out in the ANSYS program to verify the analysis results of MATLAB PDE toolbox. As a result of the validation analysis, very close values were obtained.

Acknowledgements

None declared.

Funding

The authors received no financial support for the research, authorship, and/or publication of this manuscript.

Conflict of Interest

The authors declared no potential conflicts of interest with respect to the research, authorship, and/or publication of this manuscript.

References

ANSYS (2016). ANSYS Software | ANSYS. https://www.ansys.com/products/ansys-workbench

Argyris JH, Kelsey, S (1960). A generalised discourse with applications on energy principles of structural analysis including the effects of temperature and non-linear stress-strain relations. *Energy Theorems and Structural Analysis*, 960.

Bathe KJ, Wilson EL (1976). Numerical Methods in Finite Element Analysis. Prentice Hall.

Doğangün A (2020). Betonarme Yapıların Hesap ve Tasarımı. Birsen Publishing, İstanbul.

Gallagher RH (1975). Finite Element Analysis Fundamentals. Prentice-Hall, Englewood Cliffs, New Jersey.

Jones RM (2009). Deformation Theory of Plasticity. Bull Ridge Corporation.

Kasımzade AA (2018). Finite Element Method Fundamentals and Applications in Structural Mechanics. Nobel Academic Publishing.

MATLAB R2023a (2023). https://www.mathworks.com/products/pde.html

McDowell DL, Ellis R (1993). Advances in Multiaxial Fatigue. American Society for Testing and Materials, Philadelphia.

Oden JT, Sato T (1967). Finite strains and displacements of elastic membranes by the finite element method. *International Journal of Solids and Structures*, *3*(4), 471–488.

Turkish Building Earthquake Code-2018 (n.d.). Retrieved April 17, 2023, from https://www.afad.gov.tr/

Turner MJ, Clough RW, Martin HC, & Topp LJ (2012). Stiffness and Deflection Analysis of Complex Structures. *Journal of the Aeronautical Sciences*, *23*(9), 805–823.

UNE EN 1992-1-2:2011/A1:2021 Eurocode 2: (n.d.). Retrieved April 17, 2023, from https://www.en-standard.eu

Zienkiewicz OC (1972). Finite Element Method in Engineering Science. McGraw-Hill Inc., USA.